Molecular mechanism of basal CYP3A4 regulation by hepatocyte nuclear factor 4 alpha: evidence for direct regulation in the intestine

Heike Tegude, Anke Schnabel, Ulrich M. Zanger, Kathrin Klein, Michel Eichelbaum and

Oliver Burk

Dr. Margarete Fischer-Bosch-Institute of Clinical Pharmacology, Stuttgart and University

Tuebingen, Germany

1

Running title: HNF4α regulation of intestinal CYP3A4

Oliver Burk, Ph.D.

Dr. Margarete Fischer-Bosch-Institute of Clinical Pharmacology,

Auerbachstrasse 112,

D-70376 Stuttgart,

Germany.

Phone: +49 (0)711 8101 3753

Fax: +49 (0)711 85 92 95

E-mail: oliver.burk@ikp-stuttgart.de

Number of text pages: 33

Number of Tables: 0

Number of figures: 8

Number of references: 31

Number of words in the Abstract: 248

Number of words in the Introduction: 711

Number of words in the Discussion: 1495

Abbreviations: CYP, cytochrome P450; PXR, pregnane X receptor; CAR, constitutive androstane receptor; HNF, hepatocyte nuclear factor; DR, direct repeat; XREM, xenobiotic-responsive enhancer module; CLEM4, constitutive liver enhancer module of CYP3A4; kb, kilobase pair(s); ER, everted repeat; bp, base pair(s); COUP-TF, chicken ovalbumin upstream promoter transcription factor.

Abstract

Cytochrome P450 3A4 plays an outstanding role in the metabolism of clinically used drugs and shows a marked interindividual variability in expression even in the absence of inducing agents. Thus, regulation of basal expression contributes considerably to variability. The nuclear receptor HNF4α was previously shown to be associated with basal hepatic CYP3A4 expression. As it still remains elusive how HNF4α regulates basal expression of CYP3A4, we systematically screened 12.5 kb of the CYP3A4 5´ upstream region for activation by the receptor in the human intestinal cell line LS174T. In this study, we newly identified two widely separated regions mediating the activation by HNF4α: a far distal region at -9.0 kb and the proximal promoter region around -0.2 kb. By gel shift experiments and transient transfections, we characterized DR1 type motifs in both regions as functional HNF4α response elements. Cooperation of the two regions was shown to be required for maximal activation by HNF4α. The effect of HNF4α was antagonized by COUP-TFII, which was shown to bind to one of the DR1 motifs. Furthermore, activation of CYP3A4 via the DR1 element in the proximal promoter depends on an additional, yet unknown factor, which is binding around position –189 bp. Physiological relevance of this position for activation by HNF4α *in vivo* is suggested by the presence of a similar binding activity in small intestine as in LS174T cells. In summary, we here have elucidated a molecular mechanism of direct regulation of CYP3A4 by HNF4α, which is probably specific for the intestine.

Cytochrome P450 enzymes play a pivotal role in the metabolism of many endogenous compounds as well as in the detoxification or bioactivation of xenobiotic substances and drugs. Among the human drug metabolizing cytochrome P450 enzymes, cytochrome P450 (CYP) 3A4 is of outstanding importance, as it metabolizes at least 50% of all clinically used drugs and is the isoform most abundantly expressed in liver and intestinal epithelium. It was shown to represent 40% of total hepatic and even 80% of total intestinal cytochrome P450s (Shimada et al., 1994; Paine et al., 2006).

CYP3A4 shows a pronounced interindividual variability in expression and activity (Özdemir et al., 2000; Wilkinson, 1996; Wolbold et al., 2003). In part, this variability is caused by induction of CYP3A4 expression, which depends on activation of the nuclear receptors pregnane X receptor (PXR, NR1I2) and constitutive androstane receptor (CAR, NR1I3). These xenosensors are activated by endogenous compounds (e.g. steroid hormones, bile acids) and xenobiotics including synthetic drugs (e.g. synthetic glucocorticoids, rifampin, phenobarbital) and natural products, which act as agonistic ligands of PXR or which promote the nuclear translocation of the constitutively activated CAR (for a review, see Chang and Waxman, 2006). Besides their role in mediating the induction of CYP3A4 gene expression by xenobiotics (Luo et al., 2004), PXR and CAR may also be involved in regulation of the constitutive expression of CYP3A4, as they are significantly correlated with CYP3A4 mRNA levels in liver (Wolbold et al., 2003; Pascussi et al., 2001). These data further demonstrate that induction may not be the sole source of variability, as even the basal expression of CYP3A4 varies significantly between individuals (Wolbold et al., 2003). Thus, the transcriptional regulation of basal CYP3A4 gene expression has also to be elucidated to better understand the interindividual variability in CYP3A4 expression, which in turn can be anticipated to be a major factor for variable drug response.

Another member of the nuclear receptor superfamily, hepatocyte nuclear factor (HNF) 4 alpha (HNF4α, NR2A1), has recently been identified as a prominent regulator of hepatic CYP3A4.

Expression of HNF4α antisense RNA in primary human hepatocytes resulted in 50% reduction of CYP3A4 mRNA expression levels (Jover et al., 2001). HNF4α is primarily expressed in liver, intestine, kidney and pancreas (Drewes et al., 1996) and amongst others directly regulates the expression of genes involved in the metabolism of amino acids, fatty acids, glucose and cholesterol (Sladek and Seidel, 2001). The receptor binds exclusively as a homodimer to sequence specific DNA elements, which represent divergent direct repeat (DR) 1 and DR2 types of the canonical hexameric nuclear receptor half site RGGTCA, in the 5´ upstream regulatory region of its target genes. The constitutive transcriptional activity of DNA-bound HNF4α is explained by the ligand-independent interaction with coactivators, such as steroid receptor coactivator 1 (Sladek et al., 1999). Moreover, HNF4α seems to participate in the transcriptional regulation of PXR (Li et al., 2000).

In recent years, two studies have touched on the molecular mechanism of the regulation of hepatic CYP3A4 by HNF4α, however a systematic analysis has not been performed yet. The first study (Tirona et al., 2003) showed that HNF4α modulates the responsiveness of the CYP3A4 promoter towards PXR and CAR via a DR1 element within the xenobiotic responsive enhancer module (XREM), which had first been identified as one of the two regulatory regions mediating induction by xenobiotics (Goodwin et al., 1999). Later on, binding sites for several liver-enriched transcription factors, among them two HNF4α binding sites, were identified in the far distal constitutive liver enhancer module of CYP3A4 (CLEM4). This enhancer was shown to be crucial for the constitutive expression of CYP3A4 in the hepatoma cell line HepG2 (Matsumara et al., 2004). To the best of our knowledge, an analysis of the regulation of intestinal CYP3A4 by HNF4α has never been performed.

Our study was aimed to systematically analyze HNF4α-dependent regulation of basal CYP3A4 expression. By use of transient transfection and electrophoretic mobility shift assays we identified two previously unknown DR1 motifs, widely separated in the CYP3A4 5´

upstream sequence, to which HNF4α was binding directly and which proved to be necessary, but not sufficient for HNF4α-dependent activation of CYP3A4 in the intestinal cell line LS174T. The results obtained, provide evidence for a direct regulation of CYP3A4 by HNF4α, at least in the intestine.

Methods

Human Tissue Samples

Normal human liver tissue samples were obtained from patients of Caucasian origin who underwent liver surgery at the Department of Surgery, Charité, Campus-Virchow-Clinic, Humboldt University, Berlin, Germany. The samples have previously been used and described in detail (Wolbold et al., 2003). Only samples from patients who did not receive any medication known to modulate CYP3A expression *in vivo* or *in vitro* were included into the analysis. Thus, pre-surgical treatment of patients with carbamazepine, glucocorticoids, levothyroxine, lovastatin, metamizole, nifedipine, omeprazole, pantoprazole, simvastatin, St. John's wort, tocopherol or ursodeoxycholic acid resulted in exclusion of the corresponding samples. Likewise, samples of patients with viral infections (hepatitis B and C viruses, cytomegalovirus), alcohol abuse or cirrhosis were excluded from the analysis.

Human small intestine samples (duodenum or proximal jejunum) were obtained from patients of Caucasian origin undergoing either gastrectomy or pancreatoduodenectomy at the Department of Surgery, Robert Bosch Hospital (Stuttgart, Germany). The samples have previously been used and described in detail (Burk et al., 2002; Läpple et al., 2003; von Richter et al., 2004).

RNA Analysis and Real-time PCR

Total RNA and first strand cDNA were prepared from human tissue samples as described previously (Wolbold et al., 2003, Burk et al., 2002). PCR reactions (HNF4α, CYP3A4, CYP3A7) were set up with cDNA corresponding to 25 or 20 ng of total RNA for liver or intestine samples, respectively and the TaqMan Universal PCR Master Mix (Applied Biosystems, Foster City, CA). Expression levels of all genes were quantified by TaqMan real-time quantitative PCR using the 7500 Real-Time PCR system (Applied Biosystems). The experiments were performed according to a standard protocol for the 7500 real-Time PCR

system in a final volume of 25 µl. Assays were done in triplicate. Oligonucleotide primers and

probes were designed with the PrimerExpress software (Applied Biosystems). Primers for the

HNF4α assay were used at a final concentration of 400 nM. The probe was used at 200 nM

and labeled at 5´ with the reporter dye 6-carboxyfluorescein (FAM) and at 3´ with the

quencher dye 6-carboxytetramethylrhodamine (TAMRA). Oligonucleotides used for HNF4α

were as follows: primers 5´-ATG CTT CCG GGC TGG C-3´ (exon 3) and 5´-TTC GAG

TGC TGA TCC GGT C-3´ (exon 4) and probe 5´-CTC ATT CTG GAC GGC TTC CTT CTT

CA-3´ (exon 4/3, minus strand). Serial dilutions of linearized plasmid pcDhHNF4α (Burk et

al., 2005), containing the open reading frame of human HNF4α1 were used to create the

calibration curve, ranging from 3×10^6 to 3 copies. The CYP3A4 and CYP3A7 assays were

performed as previously described (Wolbold et al., 2003, Burk et al., 2002), using respective

cDNA plasmid calibration curves from 3×10^7 to 30 copies. The expression levels of the three

genes in liver samples were normalized with respect to the corresponding 18S rRNA level, as

determined using the TaqMan ribosomal RNA control reagents (Applied Biosystems) and

serial dilutions of Caco-2 cDNA for the calibration curve. CYP3A4 and HNF4α expression

levels in intestine samples were normalized with respect to the expression levels of villin,

which were assayed as described previously (Burk et al., 2002).

Plasmid Constructs

A human bacterial artificial chromosome (BAC) library was screened by Genome Systems

(St. Louis, MO) with a 1.1 kb fragment of the CYP3A4 promoter region, which was derived

from pGL3-CYP3A4(-1105) (Hustert et al., 2001). The identified BAC clone 23577 (Genome

Systems control number 90/D7) was used for subcloning of the CYP3A4 5´ upstream region

into the reporter gene vector pGL3-Basic (Promega, Madison, WI) by a combination of

standard subcloning procedures and PCR. The resulting plasmid p-12.5kb-3A4 encompasses

the 5´ upstream region of CYP3A4 from -12.5 kb to +51 bp with respect to the transcriptional

start site, corresponding to positions 49404 to 61984 of GenBank accession number AF280107. A series of unidirectional deletions of p-12.5kb-3A4 was subsequently generated. The following positions in bp of AF280107 (restriction sites, if applicable) mark the 5′ ends of the indicated constructs: position 51467 (*Bam*HI), p-10.5kb-3A4; position 53096, p-8.8kb-3A4; position 53909 (*Apa*I), p-8.0kb-3A4; position 55932 (*Eco*RI), p-6.0kb-3A4; position 58740 (*Kpn*I), p-3.2kb-3A4. pGL3-CYP3A4(-1105) (Hustert et al., 2001), referred to as p-1.1kb-3A4 herein, was used to create constructs p-0.374kb-3A4, p-0.192kb-3A4 and p-0.136kb-3A4 by unidirectional deletion with the double-stranded nested deletion kit (Amersham Pharmacia, Freiburg, Germany). The 5′ ends of the respective deletion constructs were determined by sequencing.

The distal 5′ upstream sequence of CYP3A4 between -10.5 kb and -8.8 kb was subfragmented using PCR and restriction enzyme digests. The respective fragments were subcloned into pGL3-Basic, in front of the proximal promoter region (-364 to +51) of CYP3A4. The identity of all fragments generated by PCR was verified by sequencing.

The internal deletion of bases –250 to –210 of the CYP3A4 promoter was performed by a sequential PCR strategy according to standard procedures. Mutation of the proximal everted repeat (ER) 6 motif has been described previously (Hustert et al., 2001). Site-directed mutagenesis of the HNF4α binding sites DR1(I), DR1(II) and deletion of DR1(III) were performed by using the QuikChange site-directed mutagenesis kit (Stratagene, La Jolla, CA) and appropriate primers. Introduction of the mutations and absence of any other, undesired mutations was verified by sequencing.

The construction of reporter gene plasmids containing the proximal CYP3A7 promoter (from -350 bp to +50 bp) without or with mutation of base -188 and the corresponding mutation of base -189 in CYP3A4 have been described previously (Burk et al., 2002).

The expression plasmid pcDhHNF4α, encoding human HNF4α1, has been described previously (Burk et al., 2005). The expression plasmid pcDhCOUP-TFII, encoding human

9

COUP-TFII was generated by cloning the XbaI/KpnI 1.5 kb full length cDNA fragment of pFLCOUP-TFII (kindly provided by M.J. Tsai, Baylor College of Medicine, Houston, TX) into pcDNA3.1(-) (Invitrogen, Carlsbad, CA).

Cell Culture, Transient Transfections and Reporter Gene Assays

The human colon adenocarcinoma cell line LS174T was obtained from the American Type Culture Collection (Manassas, VA and cultivated as described (Geick et al., 2001). Transient transfections were performed in 24 well plates by using 150 ng reporter gene plasmid, 20 ng ß-galactosidase reference plasmid pCMVß (BD Biosciences Clontech, Palo Alto, CA) and 10 ng pcDhHNF4α or empty expression vector pcDNA3 (Invitrogen), filled up to a total amount of 200 ng of DNA/well with pUC18 plasmid DNA. In COUP-TFII/HNF4α co-transfection experiments, 10 ng of each expression plasmid were co-transfected. Plasmid DNA was transfected by using the Effectene^{TM} transfection reagent (Qiagen, Hilden, Germany) according to the manufacturer´s recommendations. Transfections were done in triplicates. At least three independent experiments were performed, using a minimum of two different plasmid DNA preparations of each reporter gene construct. Cells were harvested 40 h after transfection and lysed with 150 µl of 1x passive lysis buffer (Promega). Luciferase and β-galactosidase assays were performed as described previously (Burk et al., 2002). To identify statistically significant differences, one way analysis of variance with Student-Newman-Keuls post-test was performed with mean values of at least three independent experiments done in triplicates using InStat version 3.05 (GraphPad Software, San Diego, CA), if not indicated otherwise in the figure legends.

Electrophoretic Mobility Shift Assays

Human HNF4α and COUP-TFII proteins were synthesized *in vitro* using the respective expression vectors and the TNT T7 Quick Coupled transcription/translation system

10

(Promega). Nuclear protein extracts of cell lines and frozen human liver samples were prepared according to a published standard method (Schreiber et al., 1989) or by using the NE-PER Nuclear and Cytoplasmic Extraction Reagents (Pierce, Rockford, IL), respectively. Enterocytes of small intestine samples were prepared and disrupted as described previously (von Richter et al., 2004) and further centrifuged at 15,000 x g, 4°C for 30 min. The resulting pellet, containing nuclei and membrane fractions, was homogenized and used as the nuclear protein fraction. Nuclear receptor response elements were generated by annealing 1 nmole each of two complementary oligonucleotides in 25 mM Tris-Cl pH 7.5, 25 mM NaCl, 5 mM $MgCl_2$ in a total volume of 200 µl. Radioactive labeling was performed by incubating 10 pmole of the annealed double-stranded oligonucleotide with 2 units of Klenow fragment and 25 µCi [α-^{32}P]dCTP in 50 mM Tris-Cl pH 7.5, 50 mM NaCl, 10 mM $MgCl_2$, 0.2 mM each of dATP, dGTP, dTTP in a total volume of 50 µl at 37°C for 60 min. The labeled double-stranded oligonucleotides were purified through ProbeQuant™ sephadex G-50 micro columns (Amersham Biosciences). Binding reactions and gel electrophoresis were performed as described elsewhere (Geick et al., 2001). Retarded complexes were quantified with the BAS1800 II phosphor-storage scanner (Fuji, Kanagawa, Japan) and AIDA software (Raytest, Staubenhardt, Germany).

Oligonucleotides for Electrophoretic Mobility Shift Assays

-237/-211wild type sense, 5'-GAT CCA TAA GAA CCC AGA ACC CTT GGA CTC CCA-3'; -237/-211wild type antisense, 5'-GAT CTG GGA GTC CAA GGG TTC TGG GTT CTT ATG-3'; -237/-211mDR1(I+II) sense, 5'-GAT CCA TAA G*TT* CCC AG*T T*CC CTT GGA CTC CCA-3'; -237/-211mDR1(I+II) antisense, 5'-GAT CTG GGA GTC CAA GGG *AA*C TGG G*AA* CTT ATG-3'; -237/-211mDR1(I) sense, 5'-GAT CCA TAA G*TT* CCC AGA ACC CTT GGA CTC CCA-3'; -237/-211mDR1(I) antisense, 5-GAT CTG GGA GTC CAA GGG TTC TGG G*AA* CTT ATG-3'; -237/-211mDR1(II) sense, 5'-GAT CCA TAA GAA

CCC AGA ACC CTT G*TT* CTC CCA-3'; -237/-211mDR1(II) antisense, 5'-GAT CTG GGA

G*AA* CAA GGG TTC TGG GTT CTT ATG-3'; DR1(II) sense, 5´-GAT CCC CAG AAC

CCT TGG ACT CCC A-3´; DR1(II) antisense, 5´-GAT CTG GGA GTC CAA GGG TTC

TGG G-3´; DR1(III) wild type sense, 5´- GAT CCG CAG AAC CTT TGC CCT AAA A-3´;

DR1(III) wild type antisense, 5´-GAT CTT TTA GGG CAA AGG TTC TGC G-3´; DR1(III)

mutated sense, 5´-GAT CCG CAG A*TT* CTT TG*T T*CT AAA A; DR1(III) mutated antisense,

5´-GAT CTT TTA G*AA* CAA AG*A A*TC TGC G; -189T sense, 5'-GAT CCG ATT GAG

TTG T*T*T ATG ATA CA-3'; -189T antisense, 5'-GAT CTG TAT CAT AAA CAA CTC

AAT CG-3'; -189G sense, 5'-GAT CCG ATT GAG TTG T*G*T ATG ATA CA-3'; -189G

antisense, 5'-GAT CTG TAT CAT A*C*A CAA CTC AAT CG-3'. Mutated bases are shown in

italics and underlined.

Results

Hepatic and intestinal mRNA levels of HNF4α and CYP3A4 are correlated

Recently it has been shown that HNF4α antisense RNA reduced the expression of CYP3A4 in cultured primary human hepatocytes (Jover et al., 2001), thereby indicating that HNF4α may participate in the regulation of hepatic CYP3A4 expression. To confirm this role of HNF4α *in vivo*, we analyzed HNF4α and CYP3A4 expression levels in a collection of human liver samples, which were derived from patients who did not receive any medication modulating the expression of CYP3A. HNF4α and CYP3A4 mRNA expression were quantified by TaqMan real-time RT-PCR. Fig. 1A shows that HNF4α and CYP3A4 mRNA expression levels were highly correlated in liver ($r_s = 0.7817$; $p < 0.0001$; $N = 77$). As both genes are also highly expressed in the intestine, a correlation analysis of intestinal CYP3A4 and HNF4α was performed. Fig. 1B shows that CYP3A4 and HNF4α expression levels in the intestine were significantly correlated ($r = 0.4664$; $p = 0.0331$; $N = 21$). These significant correlations further support the hypothesis that HNF4α is involved in the regulation of constitutive CYP3A4 expression.

Two widely separated regions in the CYP3A4 5´upstream sequence mediate activation by HNF4α in LS174T cells

To elucidate the molecular mechanism of CYP3A4 regulation by HNF4α, we performed transient co-transfection assays with a series of reporter gene constructs containing unidirectional nested deletions of the CYP3A4 5´ upstream region ranging from –12.5 kb to –0.136 kb, together with an expression plasmid encoding human HNF4α, in the human colon adenocarcinoma cell line LS174T. This cell line is characterized by a strong basal CYP3A4 promoter reporter activity, which was much higher (>100-fold) than that of the empty reporter gene vector pGL3-Basic (data not shown). Furthermore, LS174T cells demonstrate induction

of CYP3A4 by xenobiotics, due to the strong endogenous expression of PXR (Burk et al.,

2005). Fig. 2A shows that HNF4α transactivated CYP3A4 reporter gene constructs. The

longest CYP3A4 reporter gene construct which contained the CYP3A4 5´ upstream region up

to -12.5 kb was transactivated 7-fold. Activation by HNF4α dropped significantly to 3-4 fold

if the region encompassing –10.5 to –8.8 kb was deleted. Further deletion to –0.374 kb did not

change the activation by HNF4α significantly. However, if the region between –0.374 kb and

–0.192 kb was deleted, activation by HNF4α was no longer detected. This activation profile

suggests the existence of two different regions in the CYP3A4 5´ upstream sequence, which

mediate activation by HNF4α: a distal region located between –10.5 and –8.8 kb, and a

proximal between –0.374 and 0.192 kb. We also analyzed the activation of these CYP3A4

reporter gene constructs in other cell lines (HepG2, HuH7, IHH, Caco-2, Hela and COS1) and

did not observe any activation by HNF4α. In striking contrast to LS174T cells, basal

CYP3A4 promoter reporter activity was barely detectable in these cell lines (data not shown).

Next, we tried to further cut down the responsive regions. Regarding the proximal region,

deletion of bases –250 to –210 in the context of the -0.374 kb construct completely abolished

activation by HNF4α (Fig. 2B, upper part). The proximal ER6 motif, to which PXR and CAR

are binding, resides 3´ downstream adjacent to the proximal HNF4α-dependent region.

Recently it has been suggested that PXR and HNF4α have to interact at the XREM to achieve

maximal induction of CYP3A4 by xenobiotics (Tirona et al., 2003). Therefore we

investigated whether activation by HNF4α may depend on the presence of a functional

proximal ER6 motif. The upper part of Fig. 2B shows that mutation of the ER6 motif did not

exert any influence on activation by HNF4α.

To further narrow the distal region required for activation by HNF4α, we cloned the whole

region or parts of it in front of the proximal promoter up to –0.364 kb and compared the

activation of these constructs to the respective activation of reporter constructs –10.5 kb and –

0.374 kb (Fig. 2B, lower part). The construct which contained the whole distal region between

–10.5 to –8.8 kb was activated by HNF4α as efficiently as the full length –10.5 kb construct,

thereby indicating that additional parts of the CYP3A4 5´upstream regulatory region are not

required for maximal activation by HNF4α. Deletion analysis of the distal region

demonstrated that the sequences required for HNF4α activation, are located between –9.06 kb

and -8.8 kb (Fig. 2B, lower part).

The DR1 (II) element is the functional HNF4α response element in the proximal region

To identify putative HNF4α binding sites in the proximal and distal regions, a computer-aided

search was performed by using the previously described DR1-type consensus motif

RGDBYA R RGKBYN (Sladek and Seidel, 2001). We identified two potential HNF4α

binding sites in the proximal region. These two motifs overlap with one half site each. One,

which we named DR1(II), matches the consensus, whereas the other one (DR1(I)) shows a

single mismatch (Fig.3A, upper part). To analyze the impact of the two DR1 motifs in the

proximal region on binding and activation by HNF4α, we mutated both motifs together as

well as each of the motifs separately and performed gel shift and transfection analysis of the

respective oligonucleotide probes and reporter gene constructs. Fig. 3A shows the mutated

bases in the half sites of both motifs. Mutation of both half sites of DR1(I) concomitantly

destroys also motif DR1(II), because the 5´ half site of DR1(I) overlaps with the 3´ half site of

DR1(II) (Fig. 3A).

First, we analyzed HNF4α binding to the putative motifs by gel shift experiments. Fig. 3B

shows that HNF4α was binding specifically to the region encompassing the two DR1 motifs.

Binding exclusively depends on an intact DR1(II), as demonstrated by persistent binding to

the probe with the mutated DR1(I) and loss of binding to the probe with the mutated DR1(II)

(Fig. 3B, right hand part). The specificity of the binding of HNF4α to DR1(II) was further

demonstrated by the appropriate competition gel shift experiments using wild type and specifically mutated DR1 motifs as competitors (Fig. 3B).

Next, we analyzed the impact of the two DR1 motifs on activation by HNF4α. As expected, the construct mDR1(I+II) was no longer activated by HNF4α (Fig. 3C). If specifically DR1(I) was destroyed, HNF4α activation was not impaired. In contrast, specific mutation of only DR1(II), significantly reduced activation by HNF4α (Fig. 3C). In conclusion, these results demonstrate that the DR1(II) motif is the functional HNF4α response element in the proximal region.

The DR1(III) element is the functional motif in the distal region

The computer-aided search for HNF4α consensus binding motifs resulted in the identification of a single putative binding site in the distal region, which we named DR1(III) (Fig. 4A). By gel shift experiments, we demonstrated that HNF4α was binding to DR1(III) (Fig. 4A). Competition gel shift experiments confirmed the specificity of binding to DR1(III), as only the wild type and not a mutated DR1(III) motif competed for binding (Fig. 4B). Furthermore, the competition gel shift experiments demonstrated that HNF4α was binding with similar affinities to DR1(II) and DR1(III), as both motifs similarly competed for binding (Fig. 4C). Deletion of the DR1(III) motif in the construct, which contains the distal region between -9.3 kb to -8.8 kb, cloned in front of the proximal promoter up to -364 bp, resulted in a significant reduction of the activation by HNF4α in transient transfection assays (Fig. 4D), thereby indicating that DR1(III) acts as a functional HNF4α response element. However, the DR1(III) deletion mutant was still activated more strongly than the –0.374 kb construct, which contained only the proximal region.

COUP-TFII inhibits the activation of CYP3A4 by HNF4α

COUP-TFs are known to repress the transcriptional activation of many genes. These transcription factors bind to DNA preferentially via DR1 and DR2 elements and thus may compete for binding with HNF4α. By the use of gel shift experiments, we analyzed whether COUP-TFII, which is highly expressed in liver and intestine, binds to the identified HNF4α response elements within the CYP3A4 5´upstream regulatory region. Fig. 5A shows that *in vitro* COUP-TFII binds to DR1(III) of the distal region, but not to the DR1(II) element of the proximal region. Specificity of binding was demonstrated by competition gel shift experiments, which showed that only the wild type DR1(III) element competed for binding, whereas the mutated DR1(III) and wild type DR1(II) did not (Fig. 5B).

The impact of COUP-TFII on the activation by HNF4α was analyzed by co-transfection of CYP3A4 reporter genes together with HNF4α and COUP-TFII expression plasmids. Co-transfection of COUP-TFII inhibited the activation of the -0.374 kb and -10.5 kb constructs by HNF4α (Fig. 5C). Transfection of COUP-TFII alone did not significantly change CYP3A4 reporter activity (data not shown).

Position –189T of the CYP3A4 promoter is additionally required for activation by HNF4α

The DR1(II) proximal HNF4α binding site is conserved in the CYP3A7 promoter (Fig. 6A), thereby suggesting that CYP3A7 may also be activated by HNF4α. Surprisingly and in contrast to CYP3A4, the proximal CYP3A7 promoter could not be activated by HNF4α (Fig. 6B). Previously, we have shown that mutation of position -189T>G, which corresponds to -188G in the CYP3A7 promoter, strongly impaired the activation by CAR via the adjacent ER6 motif (Burk et al., 2002). Thus, we analyzed the impact of this mutation on HNF4α-dependent activation via the nearby DR1(II) motif. Fig. 6B shows that the mutation -189T>G strongly impaired the activation of CYP3A4 by HNF4α. The reciprocal mutation -188G>T in CYP3A7 gave rise to activation by HNF4α.

Mutation -188G>T is naturally occurring in CYP3A7*1C, in which the promoter region between -188/-129 is replaced by the corresponding region of CYP3A4 (Kuehl et al., 2001). CYP3A7*1C carriers demonstrate persistent high hepatic and intestinal expression of CYP3A7 in adult life (Burk et al., 2002), which therefore may depend also on activation by HNF4α. As CYP3A7 genotypes of the liver sample donors have been previously determined (Burk et al., 2002), we tested this hypothesis by looking for correlations between CYP3A7 and HNF4α expression in CYP3A7*1C carriers (heterozygotes) versus CYP3A7 wild type homozygotes. Fig. 7 shows that HNF4α and CYP3A7 expression levels were highly correlated in CYP3A7*1C carriers (r = 0.995, p = 0.0004; N = 5). In contrast, the expression levels of both genes were only weakly correlated in CYP3A7 wild type homozygous carriers (r_s = 0.3106; p = 0.021; N = 55). Individuals carrying other variant CYP3A7 promoter alleles (CYP3A7*1B, CYP3A7*1D) were excluded from the analysis.

Nuclear protein(s) of LS174T and intestine specifically bind to position -189T of CYP3A4

The essential role of position -189T for HNF4α-mediated transactivation of the CYP3A4 promoter may be explained by specific binding of a nuclear protein to the region surrounding -189T, which then has to interact in some way with the receptor. Therefore, gel shift analyses were performed with nuclear protein extracts of LS174T cells and of other cell lines, which did not demonstrate corresponding activation of CYP3A4 by HNF4α. Fig. 8A shows that of all nuclear extracts tested, only protein(s) of LS174T and HuH7 cells were specifically binding to -189T, as compared to -189G. However, the pattern of complexes seen with nuclear extracts of LS174T and HuH7 cells differed, suggesting that the proteins, which were binding, may not be identical in the two cell lines. Thus, a specific binding activity of an unknown protein to -189T in LS174T cells may explain the activation of CYP3A4 by HNF4α in this cell line.

If the mechanism of activation of CYP3A4 by HNF4α, which we have elucidated here in LS174T cells is of physiological relevance, this specific binding activity should also be found in liver and/or intestine, where we could demonstrate significant correlations of the expression levels of both genes. Fig. 8B demonstrates that a specific binding activity to -189T could be detected in nuclear protein fractions of small intestine, which seems to be identical to that of LS174T cells. Unexpectedly, given the result shown in Fig. 7, no such binding was seen with nuclear protein extracts of liver (Fig. 8B) and of primary human hepatocytes (data not shown). In conclusion, the presence of comparable binding activities to -189T, which we demonstrated to be essential for activation of CYP3A4 by HNF4α, in LS174T and small intestine suggests that the mechanism which we elucidated in LS174T cells is of physiological relevance, at least in the intestine.

Discussion

A role for HNF4α in the regulation of CYP3A4 has first been suggested by demonstrating that inhibition of the receptors transcription in primary human hepatocytes decreased the expression of CYP3A4 (Jover et al., 2001). We here have shown that HNF4α and CYP3A4 mRNA expression are significantly correlated in adult human liver samples and in human small intestine. A similar correlation has very recently been demonstrated for HNF4α and CYP3A4 in pediatric human livers (Vyhlidal et al., 2006). These correlations further provide *in vivo* evidence for a role of HNF4α in the regulation of the constitutive expression of CYP3A4 in liver and intestine. However, the precise nature of HNF4α´s role in the regulation of CYP3A4 basal expression still remains elusive. Three different, not mutually exclusive, molecular mechanisms are conceivable: First, direct regulation by HNF4α through binding to specific response elements; secondly, indirect regulation via activation of PXR expression; and thirdly, cooperation between HNF4α and PXR, requiring or not requiring binding of HNF4α to response elements in CYP3A4. Some evidence for each of the possible mechanisms can be found in published studies (see below).

Here, we have screened 12.5 kb of the CYP3A4 5' upstream region for activation by HNF4α, which represents the first systematic analysis of the molecular mechanism of HNF4α-dependent activation of CYP3A4. Our analysis in intestinal LS174T cells provides evidence for direct regulation by the receptor, as we have clearly shown that CYP3A4 promoter activity is regulated by binding of HNF4α to two DR1 motifs which are widely separated. One motif, DR1(II), resides in the proximal promoter region nearby the proximal ER6 PXR/CAR binding site, whereas the second, DR1(III), is located at -9.0 kb. Maximal activation by HNF4α requires both elements. Activation of the proximal CYP3A4 promoter via binding to DR1(II) was shown to additionally depend on position -189T to which a yet unknown nuclear protein is specifically binding. This specific binding activity was

exclusively found in LS174T cells and in small intestine, thereby providing an explanation why the effects noted with LS174T cells could not be reproduced in other cell lines (see below).

The HNF4α binding sites, which were described in previous studies, namely the DR1 in the XREM at -7.8 kb and the A- and C-sites in the CLEM4 enhancer at -11.3 kb and -11.2 kb (Tirona et al., 2003; Matsumara et al., 2004), did not mediate activation by HNF4α in our analysis, as deletions of the respective regions did not affect activation by HNF4α. This most likely reflects a tissue-specific function of HNF4α binding sites, as we have used the intestinal cell line LS174T in contrast to the other studies, which used the hepatoma cell line HepG2. In addition, a functional role of the XREM-DR1 for activation of CYP3A4 by HNF4α, as suggested previously (Tirona et al., 2003), has very recently been questioned in a study using even the same reporter construct in the same cell line (Li and Chiang, 2006). In agreement with the latter study, we also did not observe any activation of CYP3A4 reporter constructs by HNF4α in HepG2 cells (data not shown). Furthermore, we have analyzed the activation by HNF4α in the context of the natural CYP3A4 5´ upstream region. The previous studies either exclusively used artificial enhancer/promoter fusion constructs (Tirona et al., 2003) or just looked for basal promoter activities without cotransfection of HNF4α (Matsumara et al., 2004).

An indirect mechanism of HNF4α-dependent regulation of CYP3A4 is suggested by the findings that HNF4α is required for the expression of PXR (Li et al., 2000; Kamiya et al., 2003) and that PXR expression is correlated with CYP3A4 expression in liver (Wolbold et al., 2003; Pascussi et al., 2001). Thus, transfection of HNF4α expression plasmids might have increased the expression of endogenous PXR in LS174T cells, thereby resulting in the activation of CYP3A4 reporter constructs. However, we here have shown that mutation of the

proximal ER6 PXR-binding motif did not impair activation by HNF4α, which disqualifies an indirect mechanism via increased PXR levels, at least in the intestinal LS174T cells.

Previously it was shown that both nuclear receptors cooperate at the -7.8 kb XREM in the PXR-dependent induction of CYP3A4 expression (Tirona et al., 2003). However, the issue is not yet settled whether this cooperation requires binding of HNF4α to DNA, as Li and Chiang have shown that binding of HNF4α to the XREM-DR1 element is not required. These authors conclude that binding of HNF4α to the XREM-DR1 may not be important for regulation of CYP3A4 (Li and Chiang, 2006). This is confirmed by our results, which show that the XREM region is not contributing to the activation by HNF4α in the context of the natural CYP3A4 5´ upstream regulatory region.

It has been shown that the nuclear receptor COUP-TFII modulates HNF4α–dependent transactivation. This comprises inhibition of HNF4α-mediated transactivation by competition for binding, as demonstrated for the ApoCIII promoter (Mietus-Snyder et al., 1992), as well as synergistic effects of HNF4α and COUP-TFII on transactivation, as exemplified by CYP7A1 (Stroup and Chiang, 2000). Therefore it was investigated, whether COUP-TFII may also modulate the activation of CYP3A4 by HNF4α. We demonstrated binding of COUP-TFII solely to the DR1(III) element and COUP-TFII-mediated inhibition of transactivation by HNF4α which was not restricted to constructs which harbor this element. It has been shown that COUP-TFII can also repress transactivation via a DNA-binding independent mechanism called transrepression (Achatz et al., 1997). We therefore suggest that the inhibition of HNF4α-mediated activation of CYP3A4 by COUP-TFII may involve both DNA-binding dependent and independent mechanisms. Recapitulating, the ratio of HNF4α and COUP-TFII may also contribute to the interindividual variability of CYP3A4 expression.

In this study, we have further demonstrated that HNF4α differentially regulates CYP3A4 and CYP3A7 proximal promoters. In contrast to CYP3A4, the corresponding CYP3A7 promoter

was not activated by HNF4α, although the DR1(II) element is conserved. The difference in activation by HNF4α was assigned to base -189T in CYP3A4, which corresponds to -188G in CYP3A7. A yet unknown nuclear protein of LS174T cells and small intestine was binding specifically to this region, if position -189 was a T nucleotide. Mutation from T to G, which represents a change to the CYP3A7 situation, eliminated binding. A computer-aided search for transcription factor binding sites showed that the –189T>G mutation destroys a putative HNF3 binding site. However, identity of the unknown protein of LS174T cells with any of the three HNF3 proteins α, β or γ could not be shown, just as we further could not demonstrate binding of any HNF3 protein to this region of CYP3A4 (data not shown). We have previously shown that this position is also essential for activation of CYP3A4 by CAR (Burk et al., 2002). In contrast, PXR mediated induction was not affected. It was also shown that this region of the CYP3A4 promoter is essential for the induction by glucocorticoids (El-Sankary et al., 2002). Thus the unknown factor binding around position -189 bp seems to play a central role in the activation of the CYP3A4 gene by multiple nuclear receptors. Identification of this factor, which is under way in our laboratory, will greatly enhance our understanding of the complex mechanisms of CYP3A4 gene regulation.

In most individuals, CYP3A7 is down-regulated after birth and barely expressed. However, carriers of the CYP3A7*1C promoter allele, which represents the replacement of the CYP3A7 promoter region between -188 bp and -129 bp by the corresponding sequence of CYP3A4 (Kuehl et al., 2001), show a persistent high expression of CYP3A7 in adult liver and intestine (Burk et al., 2002). As we have shown that CYP3A7 and HNF4α expression are exclusively highly correlated in CY3A7*1C carriers, activation by HNF4α may contribute to the enhanced expression of hepatic CYP3A7 in individuals carrying this allele. However, we could not demonstrate a specific binding activity in extracts from liver or primary human hepatocytes to -189T. This discrepancy may be explained by different binding properties *in vitro* and *in vivo*. On the other hand, a specific binding activity, comparable to that of LS174T

23

cells was readily detected *in vitro* using small intestinal nuclear protein fractions. Alternatively, the strong correlation of hepatic CYP3A7 and HNF4α in CYP3A7*1C carriers, in contrast to CYP3A7 wild type homozygotes, may reflect an indirect regulation of CYP3A7 by HNF4α via PXR: the replacement of the region between -188 and -129 also replaced the proximal ER6 PXR response element of CYP3A7 by that of CYP3A4, which is bound by PXR with much higher affinity (Burk et al., 2002).

In conclusion, we have identified two previously unknown HNF4α binding sites in two widely separated regions within the CYP3A4 5´ upstream regulatory sequence, which mediate HNF4α-dependent transactivation. Our results support the hypothesis that HNF4α is directly regulating basal CYP3A4 expression, at least in intestine. Tissue- and cell line-specific expression of an unknown factor, which is required for the activation of CYP3A4 by HNF4α in the intestinal model system used here and which is binding around -189T, may at least partially account for the conflicting published results, regarding direct regulation of CYP3A4 by HNF4α.

References

Achatz G, Holzl B, Speckmayer R, Hauser C, Sandhofer F and Paulweber B (1997) Functional domains of the human orphan receptor ARP-1/COUP-TFII involved in active repression and transrepression. *Mol Cell Biol* 17:4914-4932.

Burk O, Arnold KA, Nussler AK, Schaeffeler E, Efimova E, Avery BA, Avery MA, Fromm MF and Eichelbaum M (2005) Antimalarial artemisinin drugs induce cytochrome P450 and MDR1 expression by activation of xenosensors pregnane X receptor and constitutive androstane receptor. *Mol Pharmacol* 67:1954-1965.

Burk O, Tegude H, Koch I, Hustert E, Wolbold R, Glaeser H, Klein K, Fromm MF, Nuessler AK, Neuhaus P, Zanger UM, Eichelbaum M and Wojnowski L (2002) Molecular mechanisms of polymorphic CYP3A7 expression in adult human liver and intestine. *J Biol Chem* 277:24280-24288.

Chang TK and Waxman DJ (2006) Synthetic drugs and natural products as modulators of constitutive androstane receptor (CAR) and pregnane X receptor (PXR). *Drug Metab Rev* 38:51-73.

Drewes T, Senkel S, Holewa B and Ryffel GU (1996) Human hepatocyte nuclear factor 4 isoforms are encoded by distinct and differentially expressed genes. *Mol Cell Biol* 16:925-931.

El-Sankary W, Bombail V, Gibson GG and Plant N (2002) Glucocorticoid-mediated induction of CYP3A4 is decreased by disruption of a protein: DNA interaction distinct from the pregnane X receptor response element. *Drug Metab Dispos* 30:1029-1034.

Geick A, Eichelbaum M and Burk O (2001) Nuclear receptor response elements mediate induction of intestinal MDR1 by rifampin. *J Biol Chem* 276:14581-14587.

Goodwin B, Hodgson E and Liddle C (1999) The orphan human pregnane X receptor mediates the transcriptional activation of CYP3A4 by rifampicin through a distal enhancer module. *Mol Pharmacol* 56:1329-1339.

Hustert E, Zibat A, Presecan-Siedel E, Eiselt R, Mueller R, Fuss C, Brehm I, Brinkmann U, Eichelbaum M, Wojnowski L and Burk O (2001) Natural protein variants of pregnane X receptor with altered transactivation activity toward CYP3A4. *Drug Metab Dispos* 29:1454-1459.

Jover R, Bort R, Gomez-Lechon MJ and Castell JV (2001) Cytochrome P450 regulation by hepatocyte nuclear factor 4 in human hepatocytes: a study using adenovirus-mediated antisense targeting. *Hepatology* 33:668-675.

Kamiya A, Inoue Y and Gonzalez FJ (2003) Role of the hepatocyte nuclear factor 4alpha in control of the pregnane X receptor during fetal liver development. *Hepatology* 37:1375-1384.

Kuehl P, Zhang J, Lin Y, Lamba J, Assem M, Schuetz J, Watkins PB, Daly A, Wrighton SA, Hall SD, Maurel P, Relling M, Brimer C, Yasuda K, Venkataramanan R, Strom S, Thummel K, Boguski MS and Schuetz E (2001) Sequence diversity in CYP3A promoters and characterization of the genetic basis of polymorphic CYP3A5 expression. *Nat Genet* 27:383-391.

Läpple F, von Richter O, Fromm MF, Richter T, Thon KP, Wisser H, Griese EU, Eichelbaum M and Kivistö K (2003) Differential expression and function of CYP2C isoforms in human intetsine and liver. *Pharmacogenetics* 13:565-575.

Li T and Chiang JY (2006) Rifampicin induction of CYP3A4 requires pregnane X receptor cross talk with hepatocyte nuclear factor 4alpha and coactivators, and suppression of small heterodimer partner gene expression. *Drug Metab Dispos* 34:756-764.

Li J, Ning G and Duncan SA (2000) Mammalian hepatocyte differentiation requires the transcription factor HNF-4alpha. *Genes Dev* 14:464-474.

Luo G, Guenthner T, Gan LS and Humphreys WG (2004) CYP3A4 induction by xenobiotics: biochemistry, experimental methods and impact on drug discovery and development. *Curr Drug Metab* 5:483-505.

Matsumara K, Saito T, Takahashi Y, Ozeki T, Kiyotani K, Fujieda M, Yamazaki H, Kunitoh H and Kamataki T (2004) Identification of a novel polymorphic enhancer of the human CYP3A4 gene. *Mol Pharmacol* 65:326-334.

Mietus-Snyder M, Sladek FM, Ginsburg GS, Kuo CF, Ladias JA, Darnell JE, and Karathanasis SK (1992) Antagonism between apolipoprotein AI regulatory protein 1, Ear3/COUP-TF, and hepatocyte nuclear factor 4 modulates apolipoprotein CIII gene expression in liver and intestinal cells. *Mol Cell Biol* 12:1708-1718.

Özdemir V, Kalowa W, Tang BK, Paterson AD, Walker SE, Endrenyi L and Kashuba AD (2000) Evaluation of the genetic component of variability in CYP3A4 activity: a repeated drug administration method. *Pharmacogenetics* 10:373-388.

Paine MF, Hart HL, Ludington SS, Haining RL, Rettie AE and Zeldin DC (2006) The human intestinal cytochrome P450 "pie". *Drug Metab Dispos* 34:880-886.

Pascussi JM, Drocourt L, Gerbal-Chaloin S, Fabre JM, Maurel P and Vilarem MJ (2001) Dual effect of dexamethasone on CYP3A4 gene expression in human hepatocytes. Sequential role of glucocorticoid receptor and pregnane X receptor. *Eur J Biochem* 268:6346-6358.

Schreiber E, Matthias P, Müller MM and Schaffner W (1989) Rapid detection of octamer binding proteins with mini-extracts, prepared from a small number of cells. *Nucl Acid Res* 17:6419.

Shimada T, Yamazaki H, Mimura M, Inui Y and Guengerich FP (1994) Interindividual variations in human liver cytochrome P-450 enzymes involved in the oxidation of drugs, carcinogens and toxic chemicals: studies with liver microsomes of 30 Japanese and 30 Caucasians. *J Pharmacol Exp Ther* 270:414-423.

Sladek FM and Seidel SD (2001) Hepatocyte nuclear factor 4α, in *Nuclear Receptors and Genetic Disease* (Burris TP and McCabe ER eds) pp 309-361, Academic Press, San Diego, CA.

Sladek FM, Ruse MD, Nepomuceno L, Huang SM and Stallcup MR (1999) Modulation of transcriptional activation and coactivator interaction by a splicing variation in the F domain of nuclear receptor hepatocyte nuclear factor 4alpha1. *Mol Cell Biol* 19:6509-6522.

Stroup D and Chiang JY (2000) HNF4 and COUP-TFII interact to modulate transcription of the cholesterol 7alpha-hydroxylase gene (CYP7A1). *J Lipid Res* 41:1-11.

Tirona RG, Lee W, Leake BF, Lan LB, Cline CB, Lamba V, Parviz F, Duncan SA, Inoue Y, Gonzalez FJ, Schuetz EG and Kim RB (2003) The orphan nuclear receptor HNF4alpha determines PXR- and CAR-mediated xenobiotic induction of CYP3A4. *Nat Med* 9:220-224.

von Richter O, Burk O, Fromm MF, Thon KP, Eichelbaum M and Kivistö K (2004) Cytochrome P450 3A4 and P-glycoprotein expression in human small intestinal enterocytes and hepatocytes: A comparative analysis in paired tissue specimens. *Clin Pharmacol Ther* 75:171-183.

Vyhlidal CA, Gaedigk R and Leeder JS (2006) Nuclear receptor expression in fetal and pediatric liver: correlation with CYP3A expression. *Drug Metab Dispos* 34:131-137.

Wilkinson GR (1996) Cytochrome P4503A (CYP3A) metabolism: prediction of in vivo activity in humans. *J Pharmacokinet Biopharm* 24:475-490.

Wolbold R, Klein K, Burk O, Nussler AK, Neuhaus P, Eichelbaum M, Schwab M and Zanger UM (2003) Sex is a major determinant of CYP3A4 expression in human liver. *Hepatology* 38:978-988.

Footnotes

Address correspondence to:

Oliver Burk Ph.D., Dr. Margarete Fischer-Bosch-Institute of Clinical Pharmacology,

Auerbachstrasse 112, D-70376 Stuttgart, Germany. E-mail: oliver.burk@ikp-stuttgart.de

Legends for Figures

Fig. 1: Hepatic and intestinal expression levels of HNF4α and CYP3A4 are correlated.

HNF4α and CYP3A4 mRNA expression were quantified by TaqMan real-time RT-PCR in a collection of 77 human liver samples not subject to any medication which modulates CYP3A expression (*A*), and in 21 human intestine samples (*B*). Expression of both genes was normalized to the corresponding expression level of 18S rRNA in liver and of villin in intestine. The Spearman rank correlation coefficient (r_s) or Pearson correlation coefficient (r) for liver or intestinal samples, respectively, and statistical significance (p) were calculated using GraphPad Prism version 4.01 (GraphPad Software).

Fig. 2: Proximal and distal regions mediate the activation of CYP3A4 by HNF4α.

A, CYP3A4 reporter genes are shown schematically on the left. Numbers indicate positions (in kb) relative to the transcriptional start site. The results of co-transfection experiments with HNF4α expression plasmid in LS174T cells are illustrated on the right. Cells were harvested and analyzed for luciferase and β-galactosidase activity. The bars show the mean activation factor (± SD) of the reporter genes by HNF4α. The activity of each reporter in the presence of empty expression vector only was designated as 1. Statistically significant differences are indicated by asterisks (**, $p < 0.01$; ***, $p < 0.001$). *B*, CYP3A4 reporter genes are shown schematically on the left. Numbers (in kb) refer to the transcriptional start site of CYP3A4. Ellipses denote the PXR and CAR binding proximal ER6 motif. *Open ellipse*, wild type; *filled ellipse*, mutated. The results of co-transfection experiments are shown on the right, as described in *A*.

Fig. 3: The DR1(II) motif is the functional HNF4α response element in the proximal region.

A, putative HNF4α binding sites in the proximal region between -250 bp and -210 bp as identified by computer-aided search for consensus motifs. The asterisk indicates deviation from the HNF4α consensus. Numbers (in bp) refer to the transcriptional start site of CYP3A4. Shown below are the mutations which were introduced into the DR1 motifs of the proximal region to generate the indicated mutated (m) CYP3A4 promoter oligonucleotides and -0.374 kb constructs. The mutated bases are underlined. wt, wild type. *B*, electrophoretic mobility shift assays using *in vitro* translated HNF4α bound to radiolabeled oligonucleotides (probe) corresponding to the CYP3A4 promoter from -237 to -211 with the indicated wild type (wt) or mutated (m) motifs. Competition assays were performed with increasing (10-, 50-, 150-fold) molar excess of the indicated unlabeled motifs as competitors. Complexes of HNF4α with the oligonucleotides are marked by an *arrow*. *C*, LS174T cells were co-transfected with the indicated CYP3A4 promoter reporter constructs and an expression plasmid encoding HNF4α. The results are presented as described in Fig. 2. wt, wild type -0.374 kb CYP3A4 construct. Statistically significant differences are indicated by asterisks (*, $p < 0.05$).

Fig. 4: The DR1(III) motif in the distal region of CYP3A4 is bound by HNF4α and contributes to HNF4α-dependent activation.

A, sequence of the putative HNF4α binding site DR1(III) in the distal region (-9.3 kb to -8.8 kb) as identified by computer-aided search for consensus motifs. The electrophoretic mobility shift assay with radiolabeled DR1(III) oligonucleotide was performed as described in Fig. 3B. *B*, competition electrophoretic mobility shift assays with radiolabeled DR1(III) as probe and the indicated unlabeled wild type or mutated (mut) motifs as competitors. The numbers indicate the n-fold molar excess to which the competitor was added. *C*, retarded complexes (shown in B) were quantified and expressed in percentage of the complex obtained in the absence of competitor. Symbols denote the competitors used: filled squares, DR1(III); filled

triangles, DR1(II); open squares, mut DR1(III). D, CYP3A4 reporter genes are shown schematically on the left. The filled ellipse denotes the DR1(III) element. Numbers indicate positions (in kb) relative to the transcriptional start site. The results of co-transfection experiments with HNF4α expression plasmid in LS174T cells are illustrated on the right and presented as described in Fig. 2. Statistically significant differences are indicated by asterisks (*, p < 0.05).

Fig. 5: COUP-TFII inhibits HNF4α-dependent activation of CYP3A4.

A, electrophoretic mobility shift assays with *in vitro* translated COUP-TFII bound to radiolabeled oligonucleotides corresponding to the indicated motifs. Complexes of COUP-TFII with the oligonucleotides are marked by an *arrow*. *B*, competition electrophoretic mobility shift assays with radiolabeled DR1(III) motif as probe and the indicated unlabeled wild type or mutated (mut) motifs as competitors. The numbers indicate the n-fold molar excess to which the competitor was added. *C*, LS174T cells were co-transfected with the indicated CYP3A4 promoter reporter constructs and expression plasmids encoding HNF4α and COUP-TFII, as stated. The results are presented as described in Fig. 2. Statistically significant differences as determined by paired t-test are indicated by asterisks (*, p < 0.05).

Fig. 6: Activation of the proximal CYP3A4 promoter by HNF4α requires position -189T in addition to DR1(II).

A, The CYP3A4 proximal promoter region (from -230 bp to -145 bp; upper sequence) and the corresponding CYP3A7 sequence (from -229 bp to -144 bp; lower sequence) are shown. HNF4α (DR1(II)) and PXR/CAR (ER6) binding sites are boxed. Bases in CYP3A7, which differ from CYP3A4, are underlined. The position -189T in CY3A4 and the corresponding nucleotide of CYP3A7 are highlighted by boldface. *B*, CYP3A4 (3A4) and CYP3A7 (3A7) promoter reporter genes are shown schematically on the left. Filled ellipse, DR1(II) common

to both genes; filled square, functional ER6 motif of CYP3A4; open square, defective ER6

motif of CYP3A7; filled circle, CYP3A4 -189/CYP3A7 -188 T; open circle CYP3A4 -

189/CYP3A7 -188 G. The results of co-transfection experiments with the indicated CYP3A

promoter reporter genes and an expression plasmid of HNF4α in LS174T cells are shown on

the right. Data are presented as described in Fig. 2. Statistically significant differences are

indicated by asterisks (**, p < 0.01; ***, p < 0.001).

Fig. 7: Correlation of HNF4α and CYP3A7 depends on CYP3A7 genotype.

HNF4α and CYP3A7 mRNA expression were quantified by TaqMan real-time RT-PCR in a

collection of human liver samples not subject to any medication which modulates CYP3A

expression. Expression of both genes was normalized to the corresponding expression level of

18S rRNA. CYP3A7 genotypes of the liver sample donors have been determined previously

(Burk et al., 2002). Correlation analyses were performed separately for CYP3A7*1C

heterozygotes (open squares) and wild type homozygotes (filled squares). The Spearman rank

correlation coefficient (r_s) or Pearson correlation coefficient (r) for wild type homozygotes

(wt) or CYP3A7*1C heterozygotes (*1C), respectively, and statistical significance (p) were

calculated using GraphPad Prism version 4.01 (GraphPad Software). The inset shows the

analysis for CYP3A7 wild type homozygotes in more detail.

Fig. 8: Differential binding of nuclear proteins of LS174T and small intestine to the region
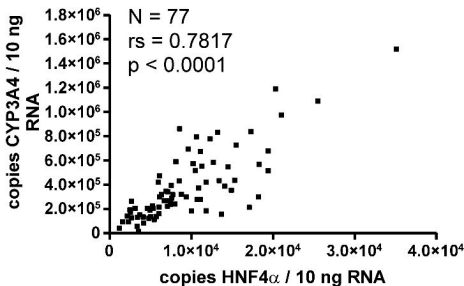
surrounding position -189.

A, electrophoretic mobility shift assays were performed with 15-20 μg of nuclear protein of

the indicated cell lines and radiolabeled double stranded oligonucleotide probes of the

CYP3A4 promoter region from -200 to -181, with T (-189T) or G (-189G) at position -189,

respectively. Complexes of nuclear proteins of LS174T cells with the-189T probe are marked

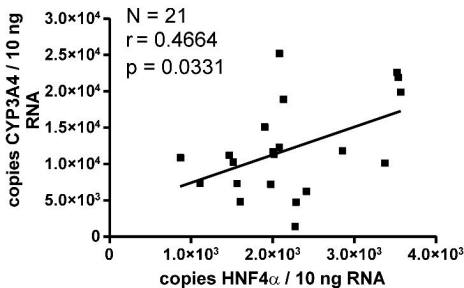by asterisks. (B) Electrophoretic mobility shift assays were performed with nuclear protein of

LS174T (lane 1), small intestine samples (lanes 2 and 3) and liver samples (lanes 4 and 5), as
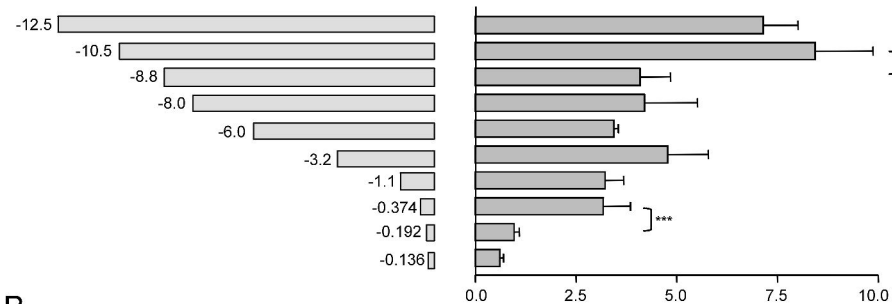
described in (A).

Fig. 1

A

N = 77
rs = 0.7817
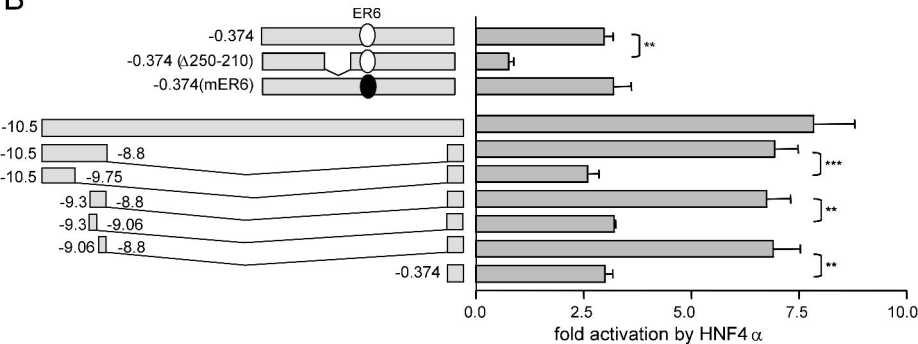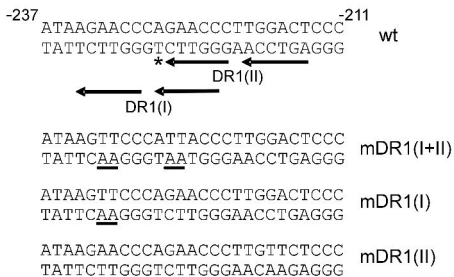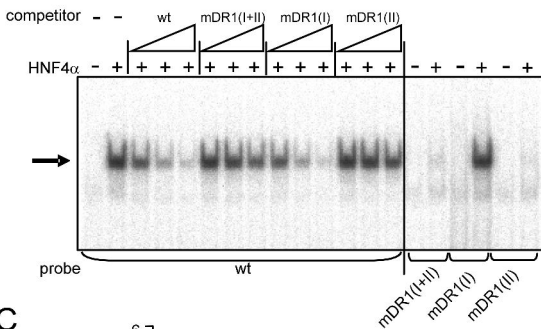p < 0.0001

copies CYP3A4 / 10 ng RNA (y-axis)
copies HNF4α / 10 ng RNA (x-axis)

B

N = 21
r = 0.4664
p = 0.0331

copies CYP3A4 / 10 ng RNA (y-axis)
copies HNF4α / 10 ng RNA (x-axis)

Fig. 2

Fig. 3

A

```
        -237                                    -211
        ATAAGAACCCAGAACCCTTGGACTCCC              wt
        TATTCTTGGGTCTTGGGAACCTGAGGG
                       *      ←━━━━━━  ←━━
                            DR1(II)
               ←━━━━━━━━━━
                  DR1(I)

        ATAAGTTCCCATTACCCTTGGACTCCC              mDR1(I+II)
        TATTCAAGGGTAATGGGAACCTGAGGG
             ‾‾       ‾‾

        ATAAGTTCCCAGAACCCTTGGACTCCC              mDR1(I)
        TATTCAAGGGTCTTGGGAACCTGAGGG
             ‾‾

        ATAAGAACCCAGAACCCTTGTTCTCCC              mDR1(II)
        TATTCTTGGGTCTTGGGAACAAGAGGG
                              ‾‾
```
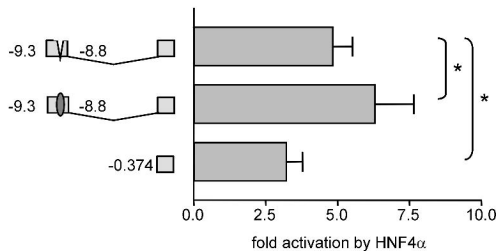
B

C

Fig. 4
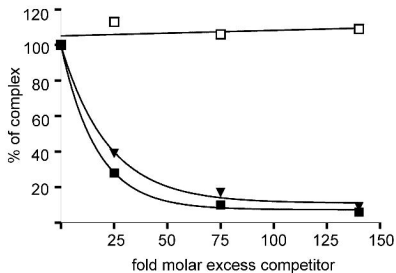
A

-9048 GCAGAACCTTTGCCCTAAA -9030
      CGTCTTGGGAAACGGGATTT
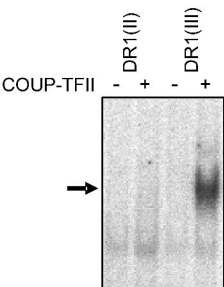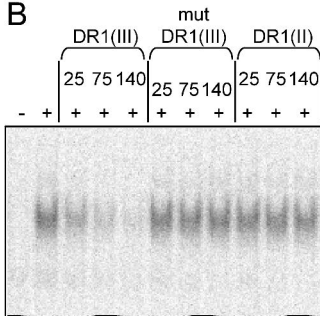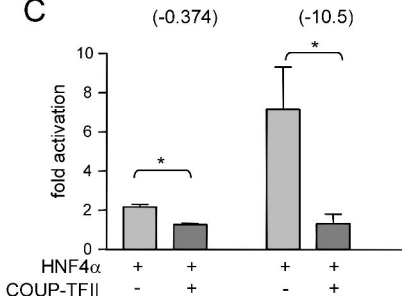
B

C

D

Fig. 5

A

DR1(II)   DR1(III)

COUP-TFII   −   +   −   +

B

                    mut
        DR1(III)   DR1(III)   DR1(II)
        25 75 140   25 75 140   25 75 140

COUP-TFII   − +   + + +   + + +   + + +

C

            (−0.374)   (−10.5)

fold activation

10 ┤
 8 ┤
 6 ┤
 4 ┤
 2 ┤
 0 ┤

HNF4α   +   +   +   +
COUP-TFII   −   +   −   +

Fig. 6

A

```
-230                                                      -189                                          -145
CCCAGAACCCTTGGACTCCCCAGTAACATTGATTGAGTTGT*TATGATACCTCATAGAATATGAACTCAAAGGAGGTCAGTGAGTG
                                          T
CCCAGAACCCTTGGACTCCCCAGTAACATTGATTGAGTTGTGTGATTCTACATAGAATATTAACTCAATGGAGGTCAGTGAGTG
-229      DR1(II)                         -188                          ER6            -144
```

B

Fig. 7

*1C
N = 5
r = 0.995
p = 0.0004

wt
N = 55
r_S = 0.3106
p = 0.021

Fig. 8

A

B